AL-Bahir
Journal for Engineering and Pure Sciences
BJEPS

Volume 8 | Issue 2 Article 8

CONDITION MONITORING OF INDUCTION MOTOR USING MOTOR CURRENT SIGNATURE ANALYSIS

Francis Ikechukwu Obianke
Department of Electrical and Electronics Engineering,DeltaStatePolytechnic,Otefe-Oghara,DeltaState,Nigeria.

Joseph Okhaifoh
Department of Electrical and Electronics Engineering,FederalUniversityofPetroleumResources,Effurun,DeltaState,Nigeria.

Benjamin Akinloye
Department of Electrical and Electronics Engineering,FederalUniversityofPetroleumResources,Effurun,DeltaState,Nigeria.

ORIGINAL STUDY

Condition Monitoring of Induction Motor Using Motor Current Signature Analysis

Francis I. Obianke [a,*], Joseph Okhaifoh [b], Benjamin Akinloye [b]

[a] Department of Electrical and Electronics Engineering, Delta State Polytechnic, Otefe-Oghara, Delta State, Nigeria
[b] Department of Electrical and Electronics Engineering, Federal University of Petroleum Resources, Effurun, Delta State, Nigeria

Abstract

Induction machines serve as the cornerstone and driving force of modern manufacturing and production systems. This research aims to monitor and analyze the operating performance of induction motors using motor current signature analysis (MCSA). MCSA is employed to process the current signal of a motor into a frequency spectrum, known as the current signature by applying the Fast Fourier Transform (FFT) algorithm. The underlying principle is that vibration generated in a motor is closely related to the changes of the magnetic field density, and the induced voltage varies with the stator current.

A simulation model replicating the behaviour of an induction motor was developed and tested under various operating conditions. Advance techniques were used for data acquisition and analysis. The results obtained from both MATLAB/SIMULINK model and the experimental setup reveal that eccentricity faults in induction motors lead to increased current draw, resulting in transient instability, non-uniform acceleration and pulsating torque due to harmonic distortion.

Keywords: Induction machine, Magnetic field density, Frequency spectrum, Eccentricity fault, Simulation, MCSA

1. Introduction

The advent of industrialization and automation has greatly enhanced the ability to monitor the condition of rotating machinery, particularly rotor bearings. Induction machines represent the foundational element in most manufacturing and production systems. For sustained and efficient production, the induction motor must remain healthy and functional. This requires regular condition monitoring, as reliance on manual assessment and routine maintenance schedules has proven inadequate [1].

In industrial environments, condition-based or on-condition maintenance strategies are increasingly adopted. Condition monitoring plays a critical role in evaluating machine health and developing predictive maintenance frameworks. The mechanical integrity of rotating machines primarily depends on the rotor bearings, which bear the load and facilitate free rotation [2]. Parameters such as acceleration, velocity, displacement and vibration frequency are essential for diagnosing and controlling the operational state of machinery. Through the analysis of these signals, maintenance strategies can be planned to extend equipment life and ensure continuous operation.

Induction motors are designed to operate within specified parameters, including power consumption, thermal limits based on insulation class, vibration frequency and load-bearing capacity determined by torque output. Deviations from these parameters often indicate developing faults [3]. The common faults in induction machines are stator, rotor and bearing faults. These faults are either electrical or mechanical fault which generate vibrations that can lead to subsystem degradation or complete machine failure.

Several techniques are employed for monitoring such faults. Displacement-based methods using

Received 30 July 2025; revised 10 November 2025; accepted 2 December 2025.
Available online 27 March 2026

* Corresponding author at: Department of Electrical and Electronics Engineering, Delta State Polytechnic, PMB 03, Otefe-Oghara, Nigeria.
E-mail address: frankobionye63@gmail.com (F.I. Obianke).

https://doi.org/10.55810/2313-0083.1131

Eddy current proximity probes and vibration sensors are cost-effective and portable but suffer from high frequency limitations and sensitivity to both electrical and mechanical noise [4]. Accelerometers are widely used due to their simplicity and accuracy in detecting high frequency faults (above 1000 Hz) [5], although they are contact-type sensors and unsuitable for direct shaft measurement. They are best suit for monitoring bearing wear and casing vibration. Laser Doppler Vibrometers (LDVs), a non-invasive type of measurement based on laser beam technology, offer precision but are very expensive and still under development [6].

This research addresses these limitations by adopting a cost-effective, on-line approach using MCSA. The objective is to develop a monitoring system capable of detecting and analysing faults in three-phase induction motors using current signatures. Specifically, it aims to compare results obtained from MATLAB/SIMULINK simulation with experimental data to assess fault severity and predict failures.

Prior studies have explored various techniques for induction motor fault detection. For instance Ref. [7], introduced a non-invasive approach using Instantaneous Power Analysis (IPA) to detect bearing faults under dynamic loads, although it was noted that integrated sensors have limited lifespans and may fail before the motor itself. Another study [8] used Fuzzy logic-based controllers and wavelet transforms to monitor eccentricity faults, demonstrating that energy levels increase with defect severity. Work in Ref. [9] applied Particle Swarm Optimization (PSO) and Artificial Neural Networks (ANNs) to detect bearing and air gap faults, though challenges remained in parameter selection and model complexity. Meanwhile [10], used Coupled magnetic circuit (CMC) modeling to simulate eccentricity faults, showing that rotor defects significantly increase torque ripple and speed fluctuations. A comprehensive review in Ref. [11] highlighted accelerometers as optimal for vibration analysis but noted the high cost of such systems.

The dynamic modelling of induction motors has received significant attention due to its importance in both performance analysis and fault diagnosis. In Ref. [12], the authors used the d-q analytical differential model analysis to modelled the eccentricity defect in 3ph induction motor and the accompanying performances. The results indicate that an eccentric motor rotor did not accelerate uniformly, instead, it exhibited intermittent glitches and flickers until it reached a maximum speed of 320 rad/s while the healthy motor accelerated uniformly from rest to maximum, rising load less speed of 0.33 rad/s. It suffered complexity and long computational time. A MATLAB model based on d-q-axis transformation in the rotor reference frame was developed in Ref. [13] to evaluate transient and steady-state behaviors of 3-phase induction motors. Their results indicated that variations in stator resistance, inertia, and load torque strongly affect the torque-speed and rotor speed-time responses, underscoring MCSA's utility for dynamic performance studies.

Building on the use of MATLAB for behavioral analysis. The authors in Ref. [14] advanced the modelling approach towards fault detection, employing the DQO stationary frame and the park vector method to characterize stator short-circuit and broken rotor bar defects. Their findings showed that healthy motors yield circular park vector patterns, whereas fault conditions distort these patterns into ellipses, thereby enabling both identification and severity assessment of defects. Also [15], advanced this modelling perspective by applying vector-based magnetic circuit equations, achieving a balance between computational accuracy and intensity for real-time control, though long computation times remained a weakness. These foundational works established the importance of accurate fault representation but underscored challenges in achieving both precision and real-time applicability.

Subsequent research shifted toward data-driven fault detection using vibration and current signatures. In Ref. [16], decision tree (DT) method was employed to analyze eccentricity faults in a 3kw induction motor, demonstrating near-perfect classification accuracy using statistical features from vibration signals. A comprehensive review of condition monitoring techniques was provided in Ref. [17], emphasizing advanced signal processing such as wavelet transform (WT), empirical mode decomposition (EMD), principal component analysis (PCA), and park's vector approach (PVA). These findings showed by these methods are highly promising for experimental deployment, though challenges included multi-sensor integration, complexity, and sensor lifespan limitations. These studies emphasized the growing role of machine learning and signal processing in improving diagnostic accuracy.

More recent works have increasingly emphasized the role of transient analysis and improved signal decomposition for MCSA-based diagnostics. Demonstrated in Ref. [18] is the utility of Hilbert and discrete wavelet transform for detecting broken rotor bars under variable load, while [19] applied autoregressive (AR) power spectral density

estimation to improve sensitivity in non-stationary conditions. These studies confirmed the diagnostic potential of MCSA beyond steady-state scenarios but also revealed the computational burden associated with such high-resolution techniques.

Despite advancements, existing condition monitoring techniques has several drawbacks from previous studies, such as noisy background/environments, Offline and Invasive procedures, Hardware dependencies and computational complexity. Sensor-based techniques in particular are constrained by sensor limited lifespan that can expire and fail.

In this work, MSCA requires no additional hard ware and uses single input source. It is non-invasive having reduced maintenance cost, precise fault detection with minimal computational overhead [20]. The novelty of this study lies on the experimental implementation. It's easy to implement and an online application that does not interrupt production. It is noise free and durable unlike sensor-based methods. The scope of the work borders around the stator, rotor and bearing faults of induction electric motor. It focuses on the eccentricity faults arising from bearing problems and its analysis.

2. Simulation and experimentation of the system

This section outlines the research methodology and parameters used for implementing and monitoring the condition of an asynchronous induction motor using motor current signature analysis (MCSA). MCSA is a versatile tool for induction motor condition monitoring, capable of accurately detecting and localizing various faults. Its evaluation metrics are influenced by system design and interface choices, while the use of MATLAB/Simulink with FFT algorithms enhances the study's robustness. It presents a comprehensive overview of the research design, data collection, simulation setup, model development, and validation process. This structured approach supports the accuracy and validity of the findings and enhances understanding of 3-phase induction motor behavior under varied operational conditions. It diagnoses motor signals by transforming them into frequency spectrum called current signature. This allows the identification of the amplitude and frequency of components within the motor's current signal, distinguishing between healthy and faulty states and locating fault occurrences.

The guiding principle is that vibration generated in an induction motor reflects changes in magnetic flux density of the motor and the voltage induced varies with the stator current. When asynchronous motor operates under faulty conditions, mechanical or electrical disturbances shift the rotor's axis, resulting in magnetic flux density variations and multiple rotational frequencies in the motor current. The MCSA in this study comprises the following steps; Signal transduction, Data acquisition, Signal processing, Fault diagnosis and detection, Fault occurrence level prediction and Failure prevention.

The flowchart (Fig. 1) illustrates the decision-making process for fault classification in an induction motor. It follows a sequence of data acquisition, preprocessing, feature extraction, and evaluation against decision thresholds to determine whether the motor has a rotor fault, bearing fault, stator fault, or is healthy.

2.1. MATLAB/Simulink model

A MATLAB/Simulink model was developed to replicate the operational characteristics of a 3-phase induction motor. This virtual model enables controlled observation of motor behavior under specified conditions and supports comparative analysis with real-world scenarios.

The model is based on a derived mathematical representation of motor's electrical and mechanical behavior.

$$I(t) = I_{st}\, sin(\ _1t + \ _s) + I_{rt}\, sin\ \bar{}\ _1t + \ \ cos\ \bar{}\ _{1f}t$$

It is implemented in the MATLAB/SIMULINK environment to generate steady-state and dynamic Simulation result.

The term $I_{st}\, sin(\ _1t + \ _s)$ result from stator MMF and it is not influenced by the torque oscillations while the term $I_{rt}\, sin\ \ _1t + \ \ cos\ \ _{1f}t$ results from the rotor MMF and presents phase modulation due to torque oscillations.

It accounts for variations in magnetic flux due to stator and rotor magnetic motive forces (MMFs), where healthy operation results in minimal fluctuations, and faults cause modulation effects in the current waveform.

Utilizing Discrete Fourier Transform (DFT) as observed from communication theory, when the motor is healthy, is null and the Bessel functions of the order n > 2 is negligible.

Therefore, applying a Discrete Fourier Transform, the Power Spectral Density (PSD) of the stator current, considering the approximations used, is given by

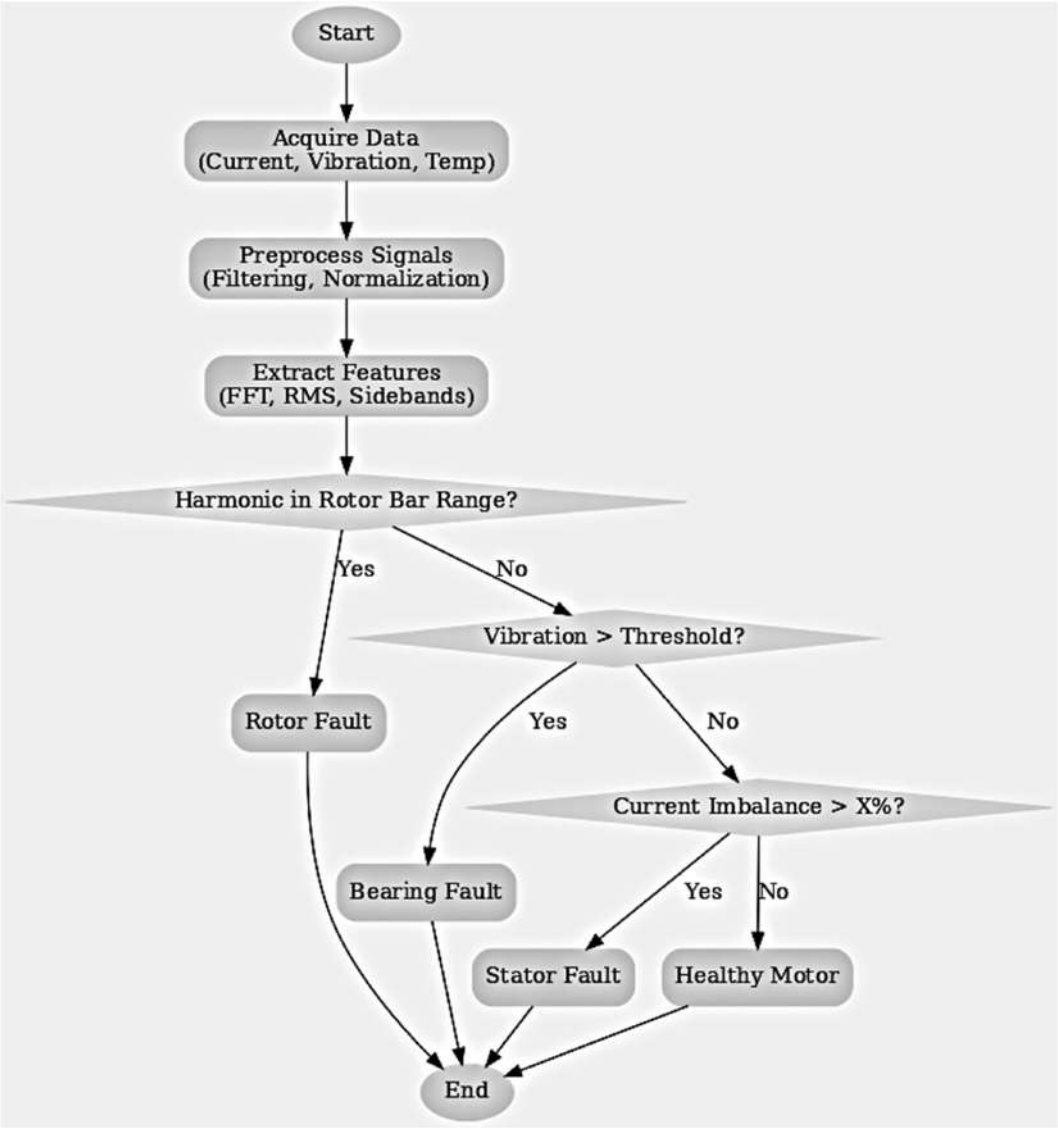

Fig. 1. Flowchart with decision-making criteria for fault classification.

$$I\bar{f} \quad = (I_{st} + I_{rt} + J_0(\ )) \quad \bar{f} - f_1 \quad + I_{rt} J_1(\ )\, f - \quad f_1 \pm f_{1f}$$

and implemented for the analysis of simulation result.

It is clear that the phase modulation leads to sideband components of the fundamental at $f_1 \pm f_{1f}$ as it happens in an amplitude modulation. These changes, driven by load torque fluctuations, create distinct frequency spectra in the current.

Fig. 2 presents the developed Simulink model, which accurately mirrors the performance of an induction motor under various fault conditions. The model's inputs include 3-phase voltage sources (Va, Vb, Vc), central frequency and load torque.

In MATLAB, essential components; voltage sources, motor starter blocks, Stator/Rotor models, fault blocks and measurement scopes, signal generators and transfer functions were assembled. The 3-phase fault block simulates eccentricity faults. Rigorous testing was conducted under three operational conditions; Healthy condition, slightly deteriorated condition and Critical faulted condition.

The fault severity is encoded within the Simulink environment using a modulation index;

0 indicates a healthy state. 0 < index <1 indicates varying degrees of fault severity.

The simulation is performed with the model operating at 75 % load because lesser load has little

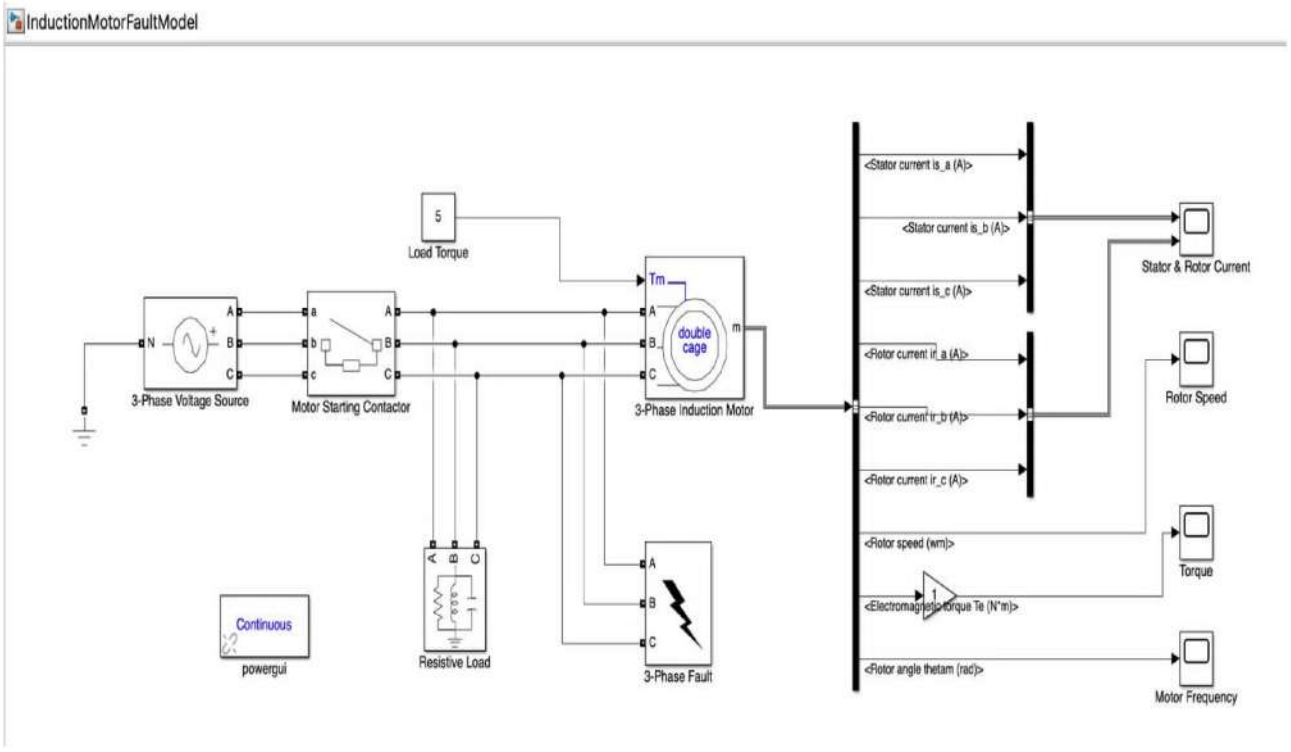

Fig. 2. The developed simulation model of the induction motor.

or no effect on the result. In each scenario, the motor performance data is recorded and analyzed.

Once the simulation model was fully developed and validated, test cases were executed for each predefined condition. The collected data were then analyzed using advanced analytical tools to detect patterns and correlations reflecting the motor's operational integrity. This data-driven approach enabled a detailed examination of discrepancies between normal and faulty motor states.

2.2. Experimental setup model

The experimental setup was designed to validate the simulation results and understand the real-world motor behavior under controlled fault conditions. It consists of both hardware and software components, as shown in Fig. 3.

The hardware components are; 3-phase induction motor, Honey well Hall-effect current transducer, Digital Oscilloscope and Data acquisition unit (DAU). while the software tools are; Computer system with MATLAB/Simulink and Fast Fourier Transform (FFT) algorithm. They are all precision and accuracy designed and implemented. The data of the asynchronous motor is shown in Table 1.

Experimental procedure;

A 3-phase power source drives the induction motor coupled with a 1.35 kw generator that acts as the load.

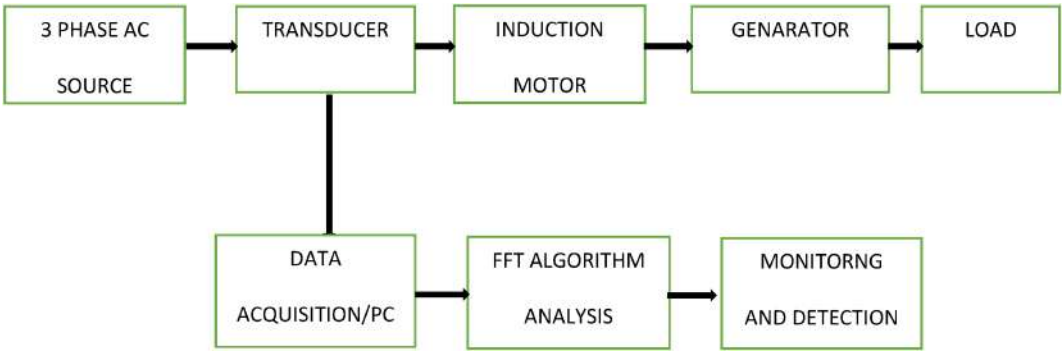

Fig. 3. Block layout of the experimental model illustrating the interfaces among the elements.

Table 1. The parameters of the 3ph induction motor.

Parameter	Ratings/values
Power Rating	2 Hp/1.5 Kw
Phase voltage Rating	380/400 V
No of poles	4
Frequency Rating	50 Hz
Stator Resistance Rs	0.85
Rotor Resistance Rr	0.23
Current Rating	5.8/3.35 Amp
Speed	1420 Rpm
Stator Inductance	0.0024 H
Rotor Inductance	0.0024 H

To simulate eccentricity faults, the motor's bearing housing diameter was increased slightly using a lathe machine, creating mechanical misalignment;

Minor fault; the motor's bearing housing was expanded by 0.4 mm while on the critical fault, the motor's bearing housing was expanded by 1.0 mm.

Motor performance was observed under both healthy and faulted states at 75 % load as the load below 75 % has negligible effect on the result.

The Hall-effect transducer with the following specification; sensitivity of 8.7 mV/A, responses time of 3 s, linearity error ± 1 to 2 % and precision; < ±0.5 % FS senses/measures the motor current and sends the signal to the Oscilloscope for amplification and filtering.

The filtered signal is digitalized using a Digital Acquisition Unit (DAU) equipped with four differential input channels and a 16-bit analog-to-digital converter (± 30 V range). The high-resolution DAU ensures precise signal capture and minimize quantization errors after which it is transmitted to a computer system for subsequent processing and analysis, thereby improving the accuracy and reliability of motor fault detection and classification.

In the MCSA, the digital signal is transformed into a frequency spectrum (current signature) using FFT-based spectral analysis with error as small as <0.01 %. As such the computational cost is significantly low thereby making it suitable for embedded monitoring platform delivery results within strict time constraints while maintaining accuracy and reliability. The integration balance cost, scalability and real-time feasibility aligning with the requirements of IoT-enabled predictive maintenance frame works. These qualities in the system architecture, design and interface strategies enhance the robust validation that makes the difference with the existing studies.

The block diagram of this experimental setup is presented in Fig. 3 while the laboratory experimental setup is shown in Fig. 4. The motor's current signature is assessed for different fault severities, highlighting changes in amplitude and frequency content. This experimental approach reinforces the simulation insights and confirms the ability of MCSA to detect motor faults accurately.

3. Result analysis

The model simulation was developed in the MATLAB environment, renowned for its robust analytical capabilities and advanced plotting functions. These tools were used to generate precise plots that illustrate the relationship between amplitude and frequency components in the motor current signatures under different operational conditions. This section compares results from the simulation model with those obtained from the physical experimental setup.

3.1. Simulation results analysis

The simulated model of a 3-phase induction motor was operated at 75 % load and subjected to dynamic eccentricity faults. Simulation data were collected

Fig. 4. Snapshot of the laboratory experimental setup.

over a 5-s time interval. Using Simulink's visualization tools, the induction motor's instantaneous current, speed, torque and frequency were plotted for three operating states; healthy, minor fault and critical fault. These are presented in Figs. 5–7.

Fig. 5 illustrates the simulation result of induction motor simulation at healthy state showing speed, current, torque, and frequency of asynchronous induction motor at 75 % load. Here, the first quarter of the graph is speed (RPM) of the motor plotted against time (secs). Second quarter current (Amp.) against time (secs). Third quarter torque (Nm) against time (secs) and forth quarter frequency (Hz) against time (secs). As the name implies healthy, the motor status is zero (modulation index $= 0$) indicating a balance magnetic pull with all the parameters operating optimally and with no fault. The current and speed are therefore stable and steady, while the torque is smooth and harmonic-free.

Fig. 6 shows the simulation result of induction motor at slightly unhealthy state illustrating the Speed, current, torque and frequency of asynchronous motor at 75 % load on minor eccentricity fault.

On the minor eccentricity fault, the motor status (modulation index) is less than 1 ($\ll 1$). Here the fault resistance is reduced to 0.5 resulting in unbalance magnetic pull that simulate slight rotor misalignment. The current draw by the motor increases slightly, acceleration becomes uneven, and torque exhibits pulsation due to harmonic distortions. The first quarter of the graph is speed (rpm) vs time (secs), second quarter is current (Amps) Vs time (secs), third quarter torque (Nm) vs time (secs) and fourth quarter is frequency (Hz) vs time (secs). (Note; This simulation ran faster than the others, slightly affecting the result).

Fig. 7 illustrates the simulation result of induction motor at critical faulty state showing the speed, current, torque and frequency of asynchronous motor at 75 % load on critical eccentricity fault. Here, the speed (rpm) in first quarter is plotted against time (secs), current (amp) in second quarter is against time (secs), torque (Nm) in third quarter against time (secs), and frequency (Hz) against time (secs). The modulation index is significantly less than 1, and fault resistance dropped to 0.01 resulting critical unbalance magnetic pull. The current consumption increases substantially to compensate the discrepancies in the motor. Acceleration becomes erratic, and torque exhibits high pulsations, indicating severe operational stress and instability. These simulation results confirm that fault severity directly impacts current draw, speed instability and torque behavior.

3.2. Experimental results analysis

The experimental validation of the asynchronous induction motor was carried out using the experimental setup previously described. The amplitude

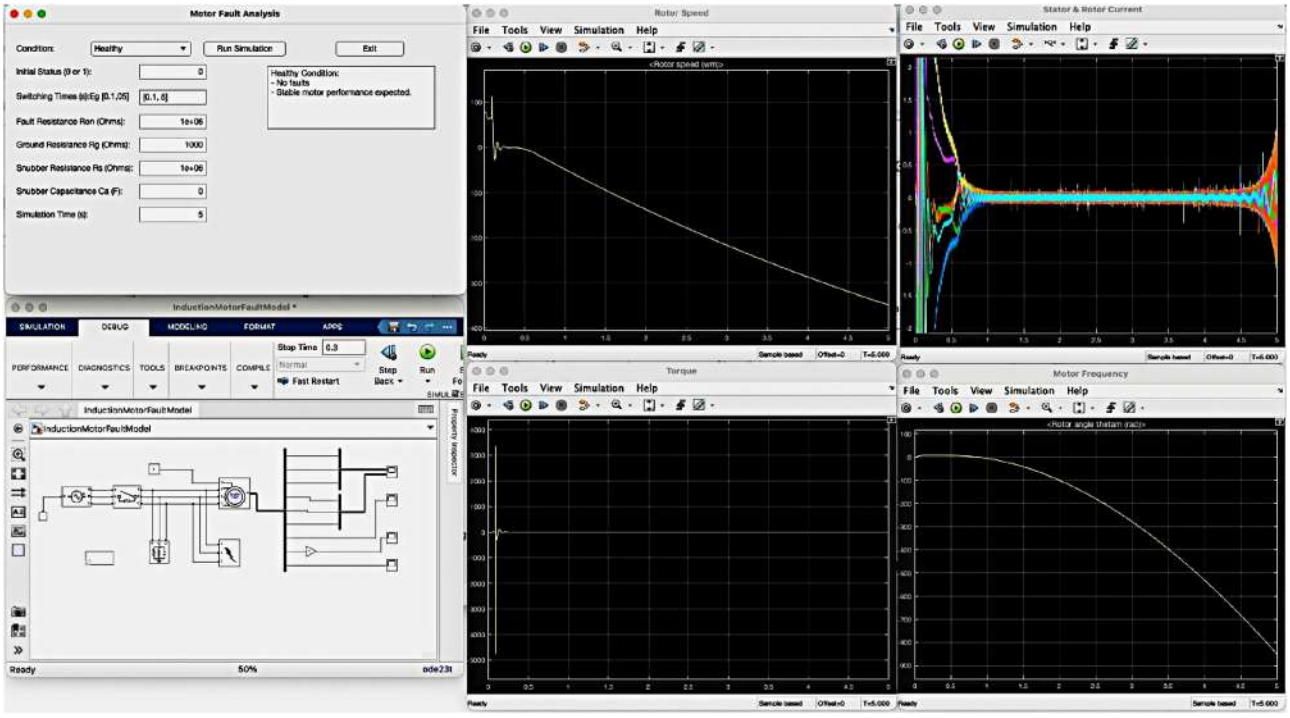

Fig. 5. Simulation result of induction motor at healthy state showing stable current, smooth torque and no harmonic distortion.

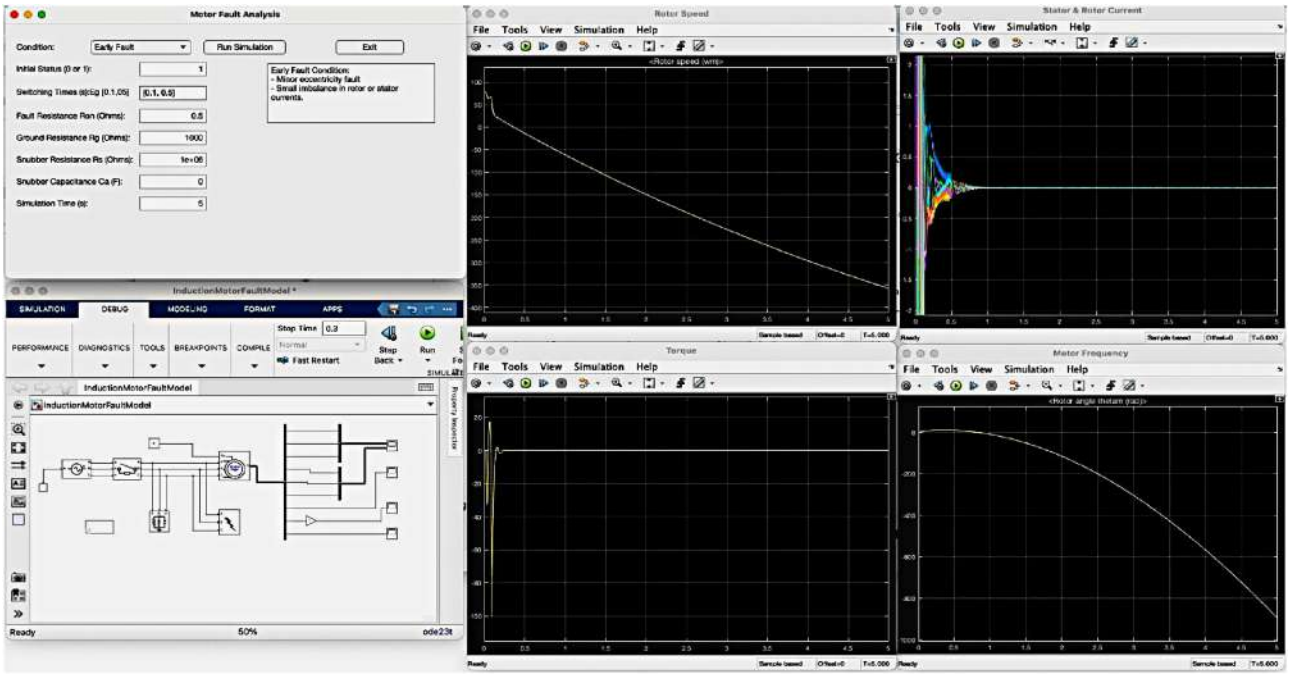

Fig. 6. The simulation result of induction motor at slightly unhealthy state.

and frequency components of the motor's current signal are captured in Table 5 for three fault states and are illustrated in bar chart and fitting curve of Fig. 8a and b.

Fig. 8 illustrates bar chart and fitting curve of induction motor operating under healthy condition at the fundamental frequency of 50 Hz, the amplitude was 10. It remained stable even when frequency

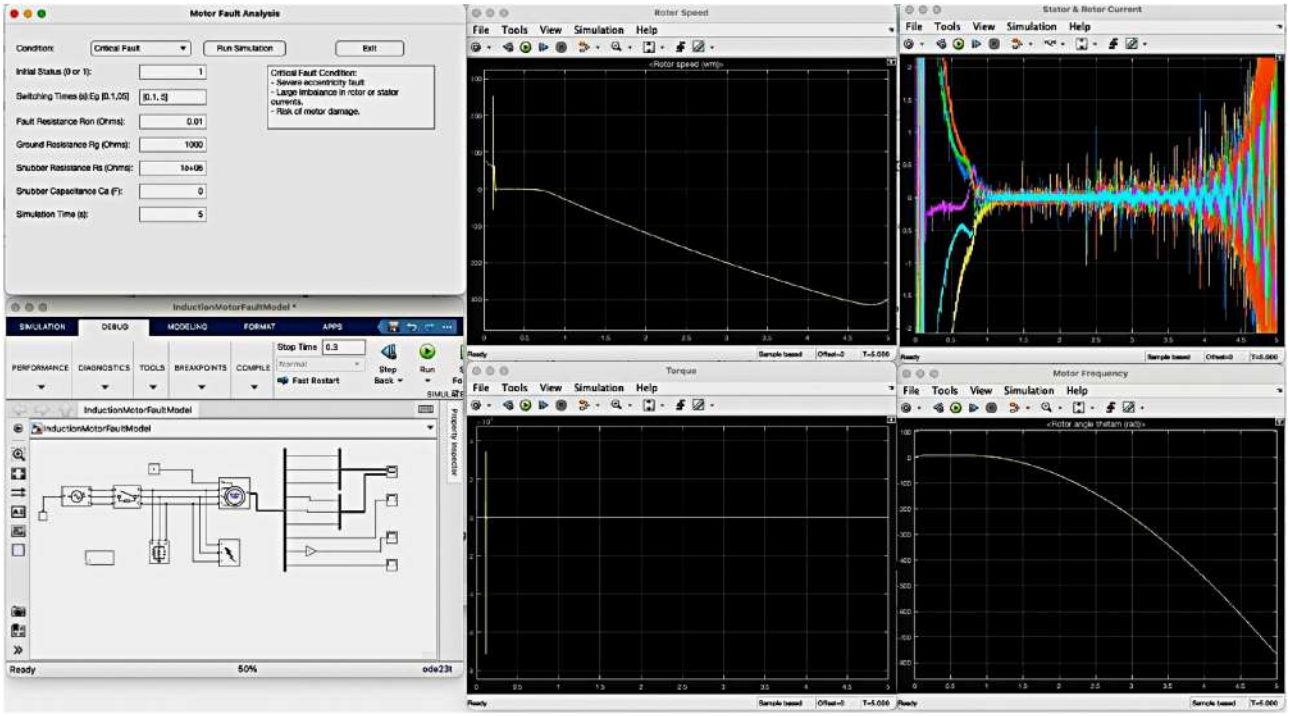

Fig. 7. The simulation result of induction motor at critical faulty stateshowing increased current, fluctuating acceleration and pulsating torque.

Table 2. Data of 3-phase induction motor on healthy condition.

Parameter	Ratings/values
Rated phase voltage	380/400 V
Initial Status (0 or 1)	0
Switching Times: Eg (0.1, 5)	(0.1, 5)
Fault Resistance Ron (ohms)	1e+06
Ground Resistance Rg (ohms)	1000
Snubber Resistance Rs (ohms)	1e+06
Snubber Capacitance Ca (F)	0
Simulation Time (s)	5

Table 3. Data of 3- phase induction motor on minor fault.

Parameter	Ratings/values
Rated phase voltage	380/400 V
Initial Status (0 or 1)	1ess than 1
Switching Times: Eg (0.1, 05)	(0.1, 0.5)
Fault Resistance Ron (ohms)	0.5
Ground Resistance Rg (ohms)	1000
Snubber Resistance Rs (ohms)	1e +06
Snubber Capacitance Ca (F)	0
Simulation Time (s)	5

Table 4. Data of 3-phase induction motor on critical fault.

Parameter	Ratings/values
Rated phase voltage	380/400 V
Initial Status (0 or 1)	1
Switching Times Eg (0.1, 05)	(0.1, 05)
Fault Resistance Ron (ohms)	0.01
Ground Resistance Rg (ohms)	1000
Snubber Resistance Rs (ohms)	1e+06
Snubber Capacitance Ca (F)	0

increased. This confirmed smooth and stable operation.

Fig. 8 illustrates bar chart and fitting curve of same asynchronous induction motor operating under minor eccentricity fault. At 50 Hz, the amplitude rose to 12.5. It increases with frequency until 150 Hz, then gradually decreased. Minor harmonics begin to appear, signaling the early stages of fault development.

Fig. 8 shows bar chart and fitting curve of same asynchronous induction motor operating under

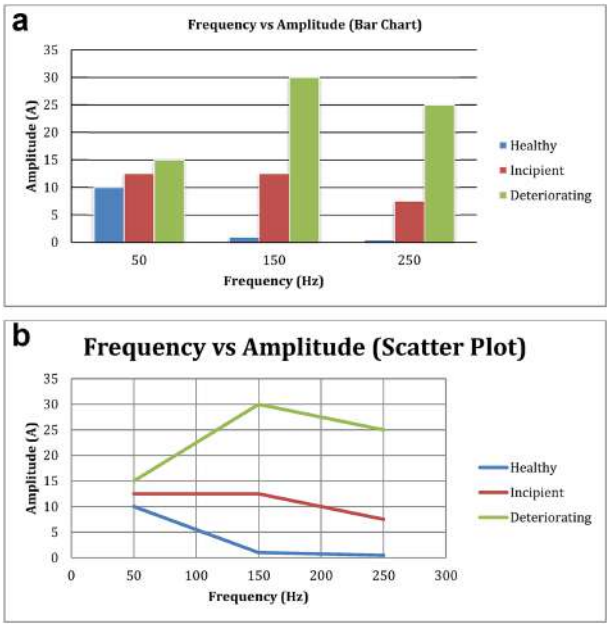

Fig. 8. a. Healthy state, Minor eccentricity Fault, and Critical Fault Condition of Asynchronous Motor in a bar chart (Note scale on the amplitude is 1:5 for clarity). b. Healthy state, Minor eccentricity Fault, and Critical Fault Condition fitting curve of Asynchronous induction motor.

critical eccentricity fault, the amplitude peaked at 15 at 50 Hz and continued to rise with frequency up to 200 Hz before decreasing. Multiple strong harmonics were present, indicating serious operational risk and significant internal damage.

The results illustrated in the simulation data of Figs. 5–7 and that of experimental set up demonstrated in Fig. 7 bar chart closely mirror the strong correlation between simulated model and experimental findings. Its variance is negligible and validates the accuracy of the MATLAB/Simulink model. The minimal variances between the datasets observed were deemed statistically insignificant, confirming the model's reliability for real-world applications.

Furthermore, the seamless integration of empirical and simulated results enhances the credibility

Table 5. Test performance of experimental setup.

Condition	Frequency (Hz)	Amplitude (A)	Observation
Healthy	50	2.0	Fundamental Frequency
	150	0.2	Negligible Harmonic
	250	0.1	Negligible Harmonic
Minor Fault	50	2.5	Fundamental Frequency
	150	2.5	Minor Harmonic; Early signs of fault
	250	1.5	Minor Harmonic; Early signs of fault
Critical Fault	50	3.0	Fundamental Frequency
	150	6.0	Significant Harmonic; Critical fault
	250	5.0	Significant Harmonic; Critical fault

of this approach, offering valuable insights for future motor diagnostic development and maintenance planning.

3.3. Statistical error analysis

Statistical results and baseline evaluation metrics for frequency-domain current signature of the induction motor across Healthy, Minor fault and Critical faults states.

A Descriptive Statistical Measure (per frequency band)

Observation; Low-frequency current (50 Hz) remain stable and consistent. Higher harmonics band (150 Hz & 250 Hz) shows large variance and strong indicators of fault progression.

B Statistical Error Analysis (Deviation from healthy state)

Minor fault Vs Healthy (Deviation measurement)
MAE (Mean Absolute Error)
$MAE = (0.5 + 2.3 + 1.4)/3 = 4.2/3 = 1.40$
MSE (Mean Square Error)
$MSE = (0.25 + 5.29 + 1.96)/3 = 7.50/3 = 2.50$
RMSE (Root Mean Square Error)
$RMSE = 1.58$
Critical fault Vs Healthy
$MAE = (1.0 + 5.8 + 4.9)/3 = 11.7/3 = 3.90$
$MSE = (1.0 + 33.64 + 24.01)/3 = 58.65/3 = 19.55$
$RMSE = 4.42$
Summary Result
Interpretation
Minor fault has moderate deviation from healthy and motor beginning to degrade.

Table 6. Input data (Current at key frequencies).

State	50 Hz (A)	150 Hz (A)	250 Hz (A)
Healthy	2.0	0.2	0.1
Minor fault	2.5	2.5	1.5
Critical fault	3.0	6.0	5.0

Table 7. Statistical measure.

Frequency	Mean (A)	Std. Dev	Min	Median	Max
50	2.50	0.5	2.0	2.50	3.0
150	2.90	2.92	0.2	2.50	6.0
250	2.20	2.52	0.1	1.50	5.0

Table 8. Deviation Measurement (minor fault).

Frequency	Fault - Healthy	Absolute difference
50 Hz	2.5 - 2.0	0.5
150 Hz	2.5 - 0.2	2.3
250 Hz	1.5 - 0.1	1.4

Critical fault shows very large deviation and severe damage or breakdown risk.

C Standard Evaluation Metrics (fault deviation perspective)

3.4. FFT analysis

The Fast Fourier Transform (FFT) analysis was conducted to evaluate the harmonic content in the current signatures under different operating conditions. The results are shown in Figs. 9–11.

Healthy Condition
Fundamental Frequency: 50 Hz
RMS Current: 7 A
Harmonics: Negligible
SNR (Signal-to-Noise Ratio in dB) $= 20\ \log10(\frac{Noise\ Amplitude}{Signal\ Amplitude})$, very high

In the healthy state, the FFT plot reveals a dominant fundamental frequency at 50 Hz with minimal harmonic distortions. This indicates stable motor operation with no structural or electrical abnormalities.

Minor Eccentricity Condition
Fundamental Frequency: 50 Hz
RMS Current: 8.2 A
Detected Sidebands: 47 Hz, 53 Hz
Harmonics: Minor

A small increase in RMS current and the emergence of sidebands around the main frequency suggest early signs of eccentricity faults. These

Table 9. Deviation measurement (Critical fault).

Frequency	Fault - Healthy	Absolute difference
50 Hz	3.0 - 2.0	1.0
150 Hz	6.0 - 0.2	5.8
250 Hz	5.0 - 0.1	4.9

Table 10. Summary of result.

Condition	MAE	MSE	RMSE
Minor fault	1.40	2.50	1.58
Critical fault	3.90	19.55	4.42

Table 11. Standard evaluation metrics.

Metrics	Interpretation
Signal Trend	As severity increases, higher frequency harmonic currents dramatically increase
Fault sensitivity (harmonic growth)	150 Hz & 250 Hz are much more sensitive to faults than 50 Hz
Signal-to-noise Ratio (SNR)	Healthy; high SNR (Minimal harmonic) Critical fault; Low SNR (Dominant harmonics)

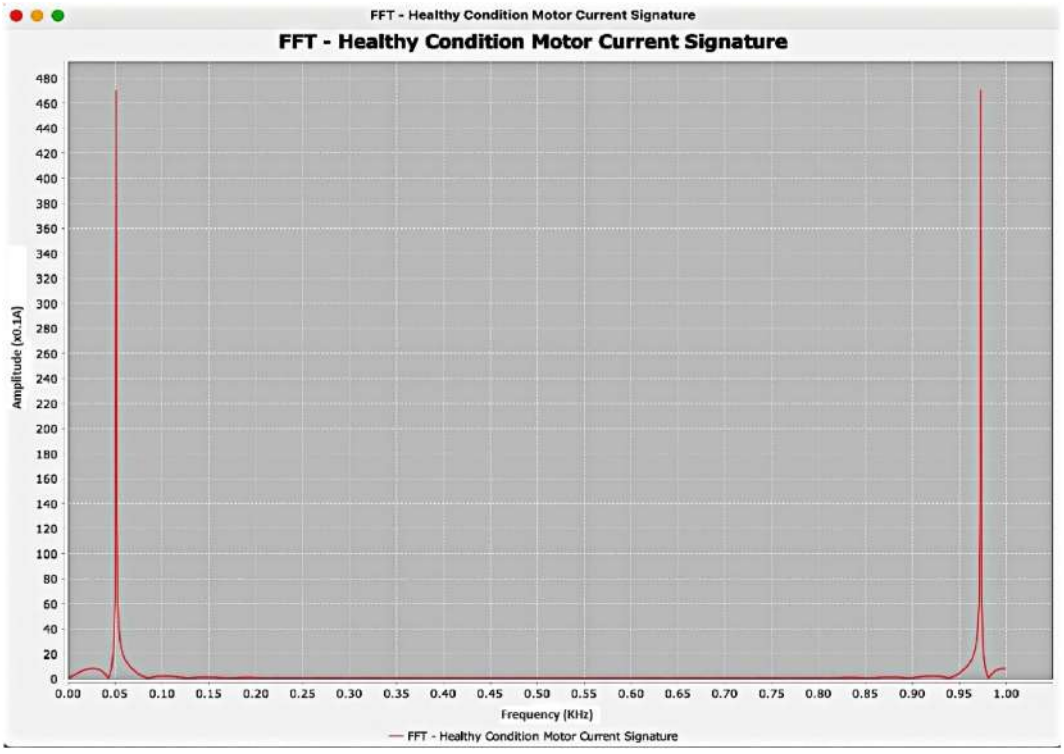

Fig. 9. Frequency spectrum of healthy motor showing harmonic free.

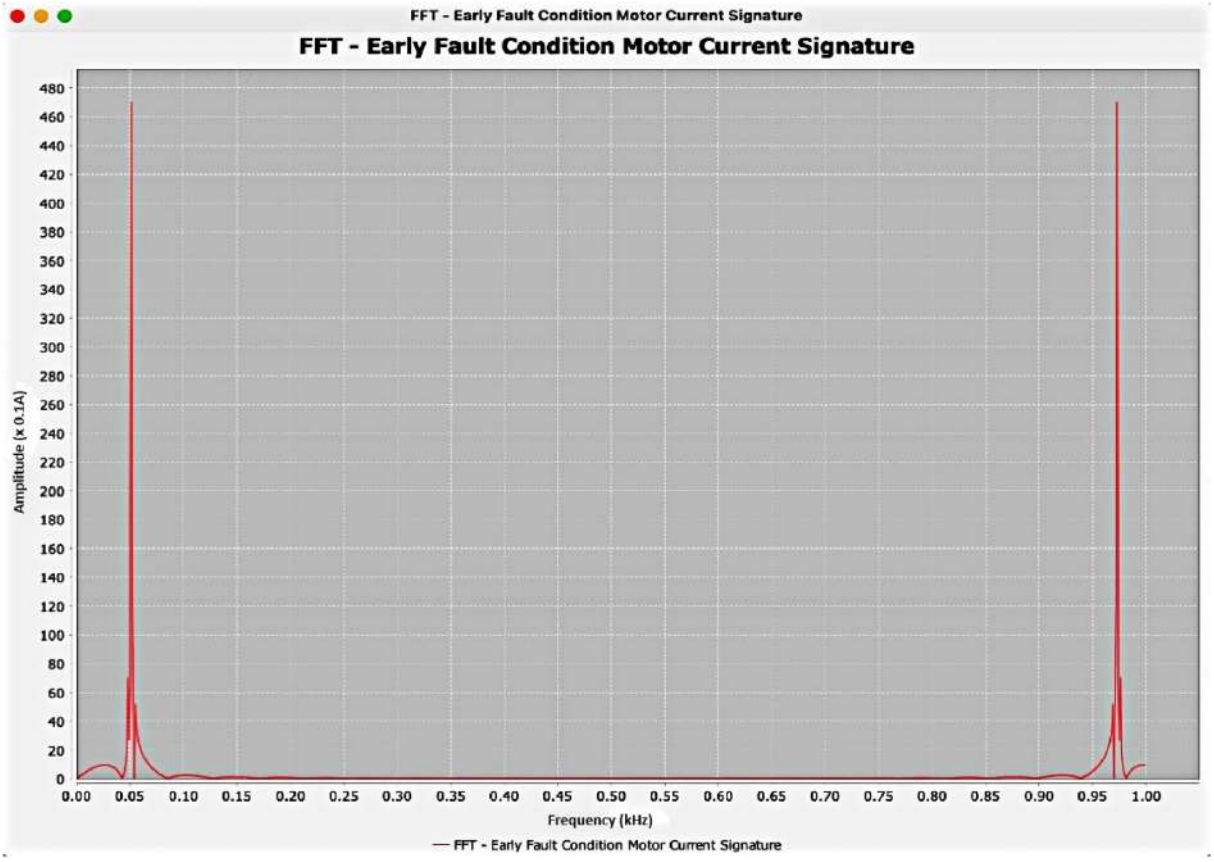

Fig. 10. Frequency spectrum of Minor eccentricity fault showing elements of harmonics.

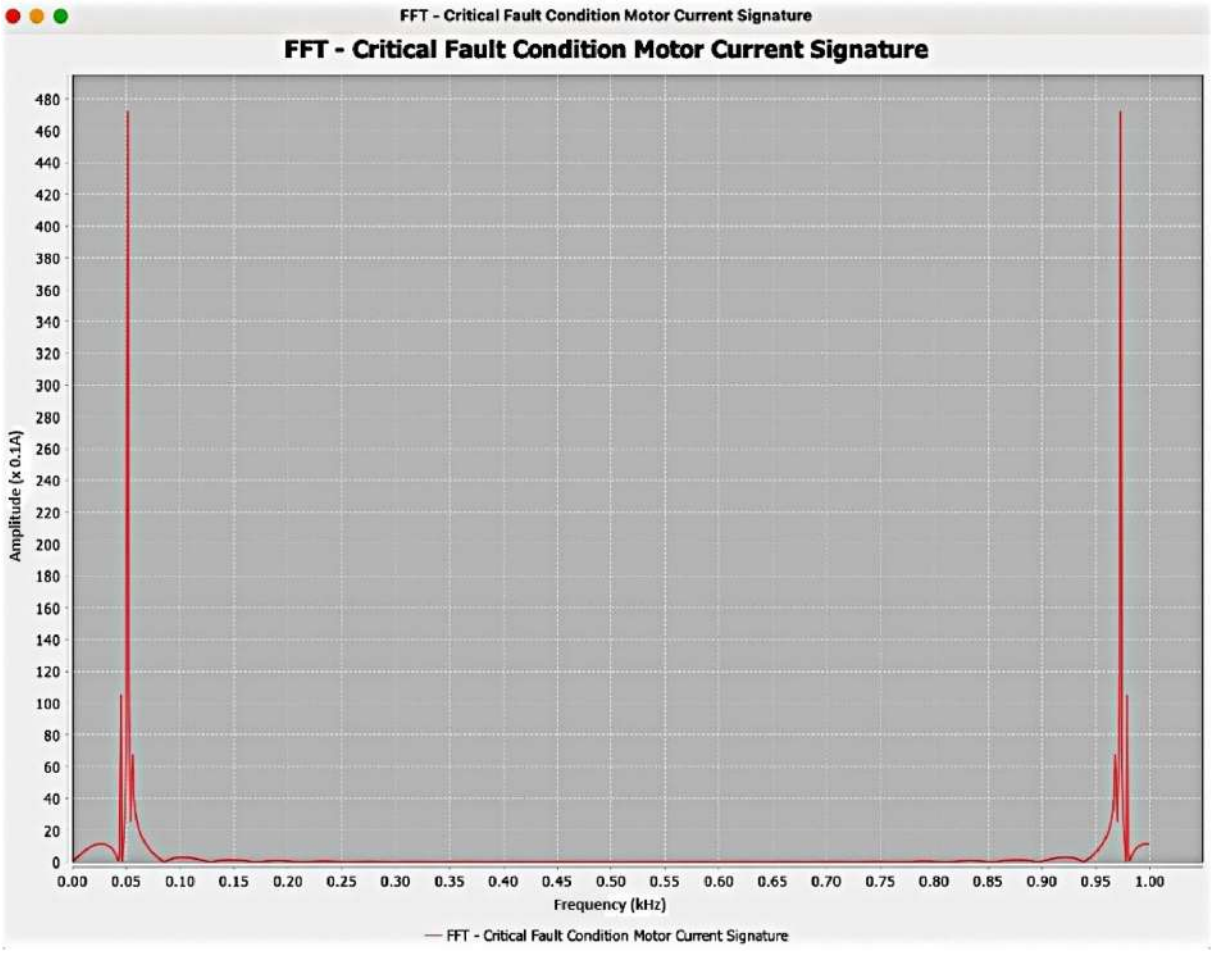

Fig. 11. Frequency spectrum of critical eccentricity fault showing harmonic due distortions.

harmonics result from unequal magnetic pull (UMP), caused by rotor-stator misalignment. For slip values above 0.01, UMP starts to grow, increasing the amplitude of specific phase windings

Critical Fault Condition

Fundamental Frequency: 50 Hz

RMS Current: 12 A

Detected Sidebands: 44 Hz, 46 Hz, 54 Hz, 56 Hz

Harmonics: Multiple and Significant

In this Condition, FFT analysis reveals substantial increases in harmonic contents and multiple significant sidebands. These features indicate severe eccentricity, with complex current patterns and significant distortions. Immediate maintenance or shutdown is required to prevent catastrophic failure.

This analytical framework using FFT proved essential in identifying and characterizing motor faults by converting time-domain signals into frequency-domain signatures. The detailed examination of sidebands and harmonics enhances fault diagnosis and supports predictive maintenance.

4. Comparative analysis and discussion

The MATLAB/Simulink-based simulation model and the experimental setup were developed, implemented, and comparatively analyzed. Results demonstrated that as fault severity increases, both the frequency and amplitude modulation of motor current become more pronounced.

This section presents the findings from both simulation and experimental investigations on the induction motor under three operating conditions: healthy state, minor eccentricity fault, and critical fault. Comparative analysis is used to evaluate the accuracy of the simulation framework and its correlation with experimentation having accuracy of ± 0.01 % to ± 0.1 % FSR and an error representation of ± 1-10 mV (<0.01%).

(i) Healthy state. The baseline condition was first examined to establish the normal operating behaviour of the motor. As shown in Fig. 4 (simulation) and Fig. 7 (experimentation), the

motor operated smoothly and steadily without any sign of instability. Both current and torque responses remained within normal limits confirming stable system performance.

The strong similarity between simulation and experimental results validates the model's ability to replicate healthy motor behaviour. This observation is consistent with prior studies that emphasized the importance of establishing a steady-state baseline for reliable fault detection [21,22].

(ii) Minor eccentricity fault. The minor eccentricity fault was introduced by reducing the fault resistance of the motor to 0.5 . The corresponding results are shown in Fig. 5 (simulation) and Fig. 7 (experimentation). This condition introduced a slight displacement in rotor alignment, resulting in an unbalanced magnetic pull. In the experimental setup, the motor exhibited increased current draw, non-uniform acceleration, and pulsating torque. These symptoms align with reported eccentricity fault characteristics in induction motors [23]. However, the simulation output deviated slightly, showing higher motor speed compared to both the healthy and critical fault cases. This inconsistency suggests that while the simulation framework successfully reproduced the general fault effects, it did not fully capture nonlinear load interactions and dynamic variations inherent in real systems. Similar limitations of modelling minor eccentricity faults have been reported in Ref. [24], where adaptive and hybrid modelling approaches were recommended.

(iii) Critical eccentricity fault. The most severe condition was observed when the fault resistance reduced to 0.01 , causing significant rotor misalignment. As illustrated in Fig. 6 (simulation) and Fig. 7 (experimentation), this fault generated a critical unbalanced magnetic pull, leading to system instability.

The motor compensated by drawing high current, which produced substantial fluctuations in acceleration and a pronounced pulsating torque dominated by harmonic distortions. Experimentally, this condition was accompanied by increased vibration levels, progressing toward instability and eventual motor failure. These observations agree with prior reports [25], where critical eccentricity faults were shown to accelerate mechanical wear due to torque ripples and harmonic-rich vibration.

Overall, the results demonstrate that both simulation and experimental studies successfully captured the characteristic signatures of eccentricity faults. The simulation framework showed strong alignment with experimental results under healthy and critical fault conditions. Minor discrepancies were observed under the minor eccentricity fault, particularly in speed prediction, which highlights the challenge of modelling weak fault signatures in purely simulation-based approaches.

Nevertheless, the experimental outcomes confirm the diagnostic capability of the proposed model. These findings reinforce the perspective of [21,26] which argue that hybrid approaches-integrating simulation, experimental validation, and IoT-based monitoring-provide a more robust pathway for accurate detection and predictive maintenance in induction motors. Efficiency and effectiveness of the system rest on the precision and accuracy of the design components employed for the experimental implementation, the findings and comparative analysis.

In the landscape of industrial applications, the fidelity of diagnostic and prognostic systems stands paramount. The FFT analysis of the stator current revealed distinct sideband frequencies associated with the specific fault. Broken rotor bars showed lower sideband frequencies around the fundamental, while eccentricity exhibited specific harmonics.

In putting side by side, the results obtained validate the capacity of MCSA to distinguish fault types based on current signal characteristics. The discussion emphasizes the advantage of MCSA in terms of low cost, ease of implementation, real-time monitoring and one understands the level of precision and consistency exuded by our computational models. Ensuring that the Simulink programmed fault severity align or tally with the experimental displacement on the induction motor stand out as a challenge in this study. Its integration into internet of things (IoT) frameworks further enhances its potential for smart industrial maintenance systems. Notably, any variance identified between simulation and real-world datasets is of minimal consequence in that challenges such as noise interference and overlapping frequency components must be addressed for broader adoption.

5. Conclusion

Motor Current Signature Analysis (MCSA) has been shown to be a versatile and effective method

for induction motor condition monitoring, capable of detecting and localizing multiple fault types. It has proven to be powerful tool for condition monitoring of asynchronous induction motors, providing critical insights into machine health by revealing anomalies in current signature patterns.

The study's contributions include developing and validating a robust MCSA-based framework that integrates MATLAB/SIMULINK with FFT algorithms for accurate fault detection and visualization. This allowed for accurate detection of fault occurrence levels and assessment of the motor's remaining operational lifespan. FFT algorithm facilitated the transformation of time-domain signals into frequency-domain representations, enabling the identification of characteristic frequencies linked to specific fault types.

Establishing the influence of system design and interface strategies on evaluation metrics such as precision, variance, and accuracy. And developing the scalability and adaptability of MCSA for potential integration with IoT-enabled monitoring systems in industrial environments.

Future work should explore advanced time -frequency techniques, AI-driven fault classification, and large-scale industrial validation to enhance robustness and applicability in industry 4.0. MCSA, a confirmed cost-effective technique is available, safe, and reliable method for real-time condition monitoring. It minimizes the need for additional hardware, simplifies implementation, and improves diagnostic precision. By enabling early fault detection and severity assessment, MCSA supports predictive maintenance strategies, reduces unplanned downtimes, extends equipment life, and enhances operational efficiency in industrial systems.

Source of Funding

This research did not receive any specific grant from funding agencies in the public, commercial, or not-for-profit sectors.

Conflicts of Interest

None.

Ethical Approval

This study was conducted in accordance with ethical standards and received approval from Federal University of Petroleum Resources Effurun, Electrical and Electronics Engineering departmental, faculty board and PG assessment committee. Informed consent was obtained from all participants prior to their involvement and all data were collected and handled with strict confidentiality. The right and privacy of the participants were fully protected throughout the research process.

Data availability statement

The data that support the findings of this study, motor current signature analysis (simulation model & experimental set up) are not publicly available due to institutional restrictions and the proprietary nature of the experimental set up. However, processed data, analysis outputs and supplementary materials used are illustrated in Tables 2–11.

Author Contributions

Author Francis Ikechukwu Obianke, did the collection of data, experimental setup/validation and the study write up.

Author Joseph Okhaifoh, did the literature review and review of the entire work.

Author Benjamin Akinloye, did the simulation and results analysis.

Acknowledgement

I wish to express my profound gratitude to the Almighty God for his infinite mercy, grace, wisdom and knowledge to carry out this programme.

My family members, my wife, Caroline and children, Emmanuel, Godswill, Esther and Chukwuemeke deserve being acknowledged and commended for their contributions, encouragement, unquantifiable support and prayers through-out the programme. May God Almighty continue to bless and preserve them all.

Special thanks to my Project Supervisor, Engr. Prof. J.E. Okhaifoh for his tireless attention. It is my prayer that the almighty God will enrich him physically, spiritually and enlarge his coast.

I appreciate my Head of Department, Engr Dr. K.O. Enalume, Engr. Prof. G. Ofualagba, Engr. Prof. G.O. Uzedhe, Engr. Prof. D.U. Onyisi, Engr. Dr. Benjamin Akinloye, Engr. Dr. E.E. Otavboruo, Engr. Dr. J. N. Onah and all the staff (academic and non-academic) in the Department of Electrical and Electronics Engineering, FUPRE, Delta State for their immense and unforgettable support and may God envelope them with his glory.

My acknowledgement also goes to my colleagues for their support, my prayer is that God will continue to shower his blessings on them all.

Finally, I wish to express my gratitude to my employer, the management of Delta State Polytechnic Otefe-Oghara for the approval, human Capital development and support of this programme.

References

[1] Sumit S Kahar, Devendra PI, Ankush IS, Subodh LN, Khan ZJ, Asutkar PG. Detection of ball bearing fault in induction motor using MCSA and harmonic analysis. World J Eng Res Technol 2020;6(4):144–58. ISSN 2454-695x.

[2] Idriss El-Thalji, Erkki Jantunen. A summary of 0888-3270/ fault modelling and predictive health monitoring of rolling element bearing. Mech Syst Signal Process 2015;60–61: 252–72. www.elsevier.com/locate/ymssphttps://doi.org/10.1016/j.ymssp.2015.02/008c 2015 Elsevier Ltd.

[3] Konstantinos Mykoniatis. A real-time condition monitoring and maintenance management system for low voltage industrial motor using internet-of-things. In: Scientific committee of the international conference on industry 4.0 and smart manufacturing, 42; 2020. p. 450–42456. https://doi.org/10.1016/j.promfg.2020.02.050.

[4] Muhammad R, Jamal, Khaled S, Rasheed AI. Vibration measurement of a rotating shaft using electrostatic sensor. Int J Recent Technol Eng 2021;10(3). ISSN: 2277-3878 (online).

[5] Courrech J, Eshleman R,L. Condition monitoring of machinery. In: Piersol AG, Paez TL, editors. Harris's shock and vibration handbook. sixth ed. New York: McGraw-Hill; 2009. Ch. 16. ISBN 978-0-07-1508193.

[6] Li Yanlu, Baets Roel. In: Nonlinear signal errors in homodyne laser Doppler Vibrometry, 29. Optical Publishing Group; 2021. p. 8283–95. 2021, 6.

[7] Muhammad Irfan, Nordin Saad, Rosdiazli Ibrahim, Vijanth S Asirvandam, Muawia, Magzoub, Hung NT. A non-invasive method for condition monitoring of induction motor operating under arbitrary loading conditions. Research article – electrical Engineering. Arabian J Sci Eng 2025. https://doi.org/10.1007/s13369-015-1996-z.

[8] Rouaibia, Reda, Arbaoui, Fay Cal 720301and Bahi, Tahar. Fault eccentricity diagnosis in variable speed induction motor drive using DWT. Amse Journals-Amse IIETA Publication, 2017-Series Advances C Vol 72 No 3 pp 181-3202, https://doi.org/10.18280/ama-C.

[9] Priyanka M, Turk N, Dahiya R. Condition monitoring of induction motor through simulation of bearing fault and air gap eccentricity fault. Int J Recent Technol Eng 2019. ISSN: 2277-3878, vol-8 issue-3. Journal website, www.ijrte.org.

[10] Yassa N, Rachek M, Housassine H. Motor current signature analysis for the air gap eccentricity detection in the squirrel cage induction machines. Emerging and renewable Energy. Energy Proc 2019;162:251–62.

[11] Mohamad Hazwan, Mohd Ghazali, Wan Rahiman. Vibration analysis for machine monitoring and diagnosis. A systematic Review, University saints, Malaysia engineering campus. 2021. https://doi.org/10.1155/2021/9469318. Ibong Tebal 14300 Wan Rahiman; wanrahiman@usm.

[12] Olaleye OS, Christopher O, Ahiakwo Dikio, Idoniboyeobu C, Sunny Orike. Modeling of eccentricity and performance of three-phase induction motors. J New Views Eng Technol (JNET) 2020;2(1):97. Available online at: http://www.rsujnet.org/index.php/publications/2020-edition.

[13] Yaabari N, Okoro OI, Akpama EJ. MATLAB-based simulation of a three-phase induction motor for dynamic studies. Niger J Technol 2022;41(6):1000–7. https://doi.org/10.4314/njt.v41i6.10.

[14] Rahmatullah R, Serteller NFO, Topuz V. Modelling and Simulation of faulty induction motor in DQ reference frame using MATLAB/SIMULINK with MATLAB/GUIDE for Educational purpose. Int J Edu Inform Technol 2023;17. https://doi.org/10.46300/9109.2023. 17,2.

[15] Kidd B. Vector-based magnetic circuit modelling of induction motors. Faculty of information technology, Monash university. Exhibition walk, Clayton, Vic Australia. Magnetism2; 2002. p. 130–51. https:/doi.org/10.3390/magnetism.

[16] Eyup, Irgat, Unsal, A., Huseyin, T. C. Detection of eccentricity faults of induction motor based on decision Trees. Ulakbim Usal - Dumlupinar University, Kutahya. Turkey. Downloaded on Jan. 22, 2022 at 21:04:14 UTC from IEEE Xplore.

[17] Rene Jaros, Radek B, Jakub D, Lukas D, Jan B, Juz K, Perk Z, Radek M. Advanced signal processing methods for condition monitoring. Arch Comput Method Eng 2023;30: 1533–77. https://doi.org/10.1007/S11831-022-09834-4.

[18] Michele Sintoni, Macrelli Elena, Bellini Alberto, Bianchini Claudio. Condition monitoring of induction machines; quantitative analysis and comparison. MDPI Sensors 2023;23:1046. https://doi.org/10.3390/s23021046.

[19] Roberto Diversi, Lenzi Alice, Speciale Nicolo, Barbieri Matteo. An autoregressive-based motor current signature analysis approach for fault diagnosis of electric motor-driven mechanisms. MDPI Sensors 2025;25:1130. https://doi.org/10.3390/s25041130.

[20] Manjeevan, Seera, Chee, Peng, Lim, Saeid, Nahavandi and Chu, Kiong, Loo. Condition monitoring of induction motors; A review and application of an ensemble of hybrid intelligent models; Published 2014 (Elsevier journal), reposted June 6, 2024 (Figshare Version 2) Journal, Expert system with applications, Vo. 41, Issue10, Pages 4891- 4903.

[21] Rahmatullah M, Kumar R, Singh D. Modeling and simulation of faulty induction motors in DQ reference frame for fault diagnosis applications. IEEE Access 2023;11:45632–44. https://doi.org/10.1109/ACCESS.2023.3261122.

[22] Yadav P, Sigh SP. Experimental validation of induction motor fault detection under healthy and faulty conditions. J Elect Eng Technol 2022;17(6):3037–49. https://doi.org/10.1007/s42835-022-01155-7.

[23] Niazi MS, Khan A, Ullah R. Minor eccentricity fault diagnosis in induction motors using motor current signature analysis and machine learning techniques. Int J Electr Power Energy Syst 2024;158:109993. https://doi.org/10.1016/j.ijepes.2024.109993.

[24] Adefarati T, Saha TK. Adaptive fault modeling for condition monitoring of induction motors under nonlinear loading. IEEE Trans Ind Electron 2023;70(5):5124–35. https://doi.org/10.1109/TIE.2023.3234567.

[25] Li X, Zhang H, Chem Y. Detection of critical eccentricity faults in induction motors using torque harmonic analysis and vibration signatures. Mech Sys Signal Proc 2023;188: 110004. https://doi.org/10.1016/j.ymssp.2023.110004.

[26] Zhou L, Wang J, Patel R. IoT-enabled hybrid condition monitoring of induction motors using vibration and current signals. IEEE Internet Things J 2025;12(3):2456–568. https://doi.org/10.1109/JIOT.2025.3345678.